

NAS3-11826

THE DYNAMIC CHARACTERISTICS OF A TURBO-ROTOR SIMULATOR
SUPPORTED ON GAS-LUBRICATED FOIL BEARINGS

Part I: Response to Rotating Imbalance and Unidirectional Excitation

by
L. Licht*



N72-12410 (NASA-CR-124620) THE DYNAMIC CHARACTERISTICS OF A TURBO-ROTOR SIMULATOR SUPPORTED ON GAS-LUBRICATED FOIL BEARINGS.
PART 1: RESPONSE TO ROTATING L. Licht
(Ampex Corp.) [1970] 40 p CSCL 13I G3/15

Unclas
06155

FACIL
CR 124620
(NASA CR OR TMX OR AD NUMBER)

63
(CODE)
15
(CATEGORY)

*Member of the Research Staff
Ampex Corporation
Redwood City, California

Reproduced by
NATIONAL TECHNICAL
INFORMATION SERVICE
Springfield, Va. 22151

1-7

CONTENTS

LIST OF FIGURES

ABSTRACT

INTRODUCTION

DESIGN OF FOIL-BEARING SUSPENSION AND OF
EXPERIMENTAL APPARATUS

INSTRUMENTATION

EXPERIMENTS

Rotation in the Horizontal Attitude and Response
to Residual Imbalance

Response to Symmetric and Asymmetric Imbalance
in the Horizontal Attitude

Rotation in the Vertical Attitude and Response to
Residual Imbalance

Response to Unidirectional Excitation by a Vibrator
(Shake-Table)

CONCLUSIONS

ACKNOWLEDGEMENTS

REFERENCES

C

LIST OF FIGURES

1. View of Foil-Bearing Supported Rotor in the Horizontal Attitude
2. View of Foil-Bearing Support Assembly
3. Schematic Diagram of Experimental Apparatus
4. Scan of Response to Remanent Imbalance in Horizontal Attitude (Increasing Speed)
5. Rotor Orbits at Major Resonances (Horizontal Attitude - Pressurized Foil Bearing)
6. Variation of Gap Width with Increasing and Decreasing Speed in Pressurized and Self-Acting Modes (Horizontal Attitude - Foil Sector B_{13})
7. Comparison of Orbits in Horizontal Attitude at Various Levels of Rotating Imbalance (Upper Orbits at 8400 RPM ~ Resonant Bandwidth; Lower Orbits at 36,000 RPM ~ Rated Speed)
8. Scan of Response to Remanent Imbalance in Vertical Attitude (Decreasing Speed)
9. Rotor Orbits at Major Resonances (Vertical Attitude - Pressurized Foil Bearing)
10. Rotor Orbits at First Overharmonic Resonances (Vertical Attitude - Pressurized Bearing)
11. Variation of Gap Width with Increasing and Decreasing Speed in the Pressurized and Self-Acting Modes (Vertical Attitude - Foil Sector B_{13})
12. Comparison of Coastdown Curves in Vertical and Horizontal Attitudes
13. View of Experimental Apparatus and Vibrator
14. Scan of Response to Unidirectional Excitation (Horizontal Attitude; $N = 36,000$ RPM; $G_x = 0.8$ g)
15. Motion of Rotor at Resonance (Horizontal Attitude; $N = 36,000$ RPM; $G_x = 0.8$ g)
16. Motion of Rotor at Various Frequencies of Excitation (Horizontal Attitude; $N = 36,000$ RPM; $G_x = 0.8$ g)
17. Response of Rotor at Variable Level of Excitation (Horizontal Attitude; $N = 600$ RPS; $f_e = 300$ CPS; $1 \leq G_x \leq 5$ g)

THE DYNAMIC CHARACTERISTICS OF A TURBO-ROTOR SIMULATOR
SUPPORTED ON GAS-LUBRICATED FOIL BEARINGS

Part I: Response to Rotating Imbalance and Unidirectional Excitation

ABSTRACT

A sixteen-inch long rotor, weighing approximately twenty-one pounds, was supported by air-lubricated foil bearings. In physical size and in mass distribution, the rotor was closely matched with that of an experimental Brayton cycle turbo-alternator unit. The rotor was stable in both the vertical and horizontal attitudes at speeds up to 50,000 rpm. A detailed description of the experimental apparatus and of the foil bearing design are given. The paper contains data of response of the rotor to rotating imbalance, symmetric and asymmetric, and to excitation by means of a vibrator (shake-table). It is concluded that the gas-lubricated foil-bearing suspension is free from fractional-frequency whirl and suffers no loss of load capacity when excited at frequency equal half the rotational speed. On contrast with rigid gas bearings, the foil bearing imposes no stringent requirements with respect to dimensional tolerances, cleanliness, or limitations of journal motion within the narrow confines of bearing clearance.

INTRODUCTION

Foil bearings are generally associated with the transport of flexible webs under tension and, specifically, with the generation of lubricating films separating foil-like materials from arrays of cylindrical guides and rollers. Whether by design or by coincidence, foil bearings have always existed in the manufacture and processing of paper, plastic and metal foil, but recent studies of foil bearings received the impetus from the development of tape transports and of devices for magnetic recording on flexible media in general. A review of these studies is beyond the scope of the present investigation, and the reader is referred to comprehensive bibliographies contained in references [1] and [2].*

With the exception of peripheral applications, such as loading devices, for example [3], no serious attempts have been made in the past to utilize foil bearings as actual supports for high-speed rotors. In the course of a recent feasibility study, however, speeds of the order 350,000 RPM were attained with a one pound, one inch diameter rotor, supported in the vertical attitude by very compliant foil bearings [4]. Rotation with preloaded foils could be initiated upon temporary flooding of bearings with liquid freon, but the experimenters found it difficult to control the foil suspension and the gyrations of the rotor.

The present study was facilitated by the results of an earlier investigation, reported in considerable detail in references [5] and [6]. The latter furnished useful results, applicable to the construction and the estimation of dynamic characteristics of the foil-bearing rotor support described in the following section. The objectives of the present study were to advance the foil-bearing concept from feasibility to practicality

*Numbers in brackets designate References at end of paper.

as means of support for high-speed turbomachines and to increase the experience necessary for incorporation of the concept in a realistic design.

The mass and moment of inertia of the rotor were closely matched with those of an existing turbo-alternator and provision was made for rotation in both the vertical, that is radially unloaded, and in the horizontal attitudes. Experiments described in the following sections pertain to responses of the foil-rotor system in both attitudes. Data ~~was~~^{were} obtained for rotation in both the pressurized and self-acting modes, with a balanced rotor and with various amounts of symmetric and asymmetric imbalance added. Additional information, relevant to the dynamic characteristics of the foil-bearing supported rotor, was derived from experiments involving excitations by means of a vibrator (shake-table).

DESIGN OF FOIL-BEARING SUSPENSION AND OF EXPERIMENTAL APPARATUS

A pictorial view of the foil-bearing supported rotor in the horizontal attitude is shown in Fig. 1. Component parts of the foil-bearing support are presented in greater detail in Fig. 2. In the description of the test apparatus, given in the following paragraphs, numbers in parentheses refer to components listed in the schematic diagram of the experimental apparatus in Fig. 3.

The 20.9 lb rotor (1) was 16 inches long and had a polar moment of inertia $I_p = 0.0595 \text{ in-lb-sec}^2$ and a transverse moment of inertia $I_t = 1.185 \text{ in-lb-sec}^2$. The rotor was symmetrical and two journal sleeves, 2.5 inches in diameter and approximately 4 inches long, were shrunk on the rotor core with a 0.002 inch interference fit at the 2 inch diameter interface. Each sleeve had 4 rows of 24 orifices, equally spaced along the periphery. Through these, compressed air was supplied from the interior of the rotor to separate the preloaded foils from the journals on starting, stopping, and at low rotational speeds. The location of orifice rows along the journals was 0.25 inch inboard from the edges of the 1.5 inch wide foils, arranged in tandem at each bearing journal.

Two end-discs, threaded into the core of the simulator, corresponded to the turbine and compressor wheels. For convenience, one of the discs was used as a thrust plate, through the center of which the hollow interior of the rotor was connected to the foil-lift pressure source. Each disc contained 18 tapped holes for adding balancing screws.

An air-driven turbine wheel (8), containing 24 milled buckets, was located at the center plane of the rotor. The entire rotor was made of AISI type 440C stainless steel, with journals hardened to C-56 Rockwell. The 2.5 inch

diameter sleeves were concentric and round within 100 μ inches, with taper the order of 50 μ inches along the 4 inch journal lengths. The surface finish of journals was 4 μ inches RMS. The moments of inertia of the rotor were determined by pendulation within an accuracy of 2% and balancing was performed on a Schenck Balancing Machine, Model RS1-b to within 350 μ in-oz. in each balancing plane.

The foil bearings (2) were similar in construction to the experimental unit described in references [5] and [6]. Each foil bearing support (3) contained clusters of symmetrically spaced guide posts (4) and foil locks (5), arranged in tandem on opposite sides of the support plates (3). The split-construction, doweled support plates were spaced 9 inches apart and securely assembled into a single frame. The 32 cantilevered foil guides, press-fitted in pairs into jig-bored holes and secured by means of tie bolts, were parallel to each other and to the reference planes of the foil-bearing support sub-assembly within 0.0002 inch. (See Fig. 2.)

The foil bearing supports straddled a turbine nozzle-ring and manifold (9), from which 8 rectangular nozzles, operating at choked flow conditions, directed air jets, at an angle calculated to generate a relatively high torque at rated speed. Adjacent to the rotor ends were two precisely machined angle plates, the thrust bearing support plate (7) and the alignment support plate (16). The foil-bearing support assembly, the thrust-bearing support, the symmetrical alignment support, and the nozzle ring were securely bolted to a sturdy 1.5 x 12 x 26-inch aluminum base (13), flat to within 0.002 inch. Spacing of the foregoing components was accomplished by means of precision gauge blocks and lateral alignment assured by using for reference a massive, precision-ground bar (10), attached to the base.

The construction of the fixed, externally pressurized thrust bearing (6) allowed for various adjustments and substitutions of components. While the investigation was focussed on the foil bearings, rather than on

the thrust bearing, the operational clearances and outer dimensions of the latter were realistic and representative. The inboard thrust member consisted of three circular, axially adjustable pads, clamped on sturdy, cantilevered rods, pressed into the thrust-bearing support plate. This arrangement permitted a great deal of flexibility in adjusting the total axial clearance. The outboard thrust member consisted of a cluster of six circular and equally spaced pressure pads, which could be easily replaced by a single, multi-orifice plate. (Shown in Fig. 3)

The annulus between a central pad and the rotating end disc provided a face seal for the foil-lift air supply, ducted through a 5/16 inch hole, concentric with the pad and the rotor axis. The seal was coplanar with the outboard thrust surface, but separated from the bearing areas and vented to the ambient atmosphere.

The inboard and outboard thrust members and the foil lift were supplied from separate and individually regulated plenums, located in the cover plate at the rear of the thrust-bearing support plate (7). The independently regulated supplies augmented the operational flexibility furnished by the adjustable thrust-bearing clearance.

The procedure followed in securing and preloading of foils was the following: The rotor weight, supported initially on alignment pins (11) slip-fitted to matching holes in the rotor end discs and in the adjacent support plates, was counterbalanced by means of levers (12). The foils were then looped around the guides, brought into intimate contact with the journals along the upper arcs of wrap and secured at the outer posts of the upper guide-clusters. Preload weights were then attached to the free ends of the foils, threaded through guides adjacent to the foil locks. Upon removal of alignment pins, the foil bearings were pressurized and depressurized to equalize the preload tension in all three foil sectors prior to securing of foil locks. The counterbalancing of the rotor before preloading was convenient and equivalent to application of initial tension in the vertical attitude. In the last step, all weights were removed, making the simulator operational.

INSTRUMENTATION

The orbital motion of the rotor was monitored by means of orthogonal capacitance probes, in the midplanes of two tandem-foil bearings, spaced 9 inches apart. Provision was made for measurement of foil displacement at the midpoints of the 60 degree regions of wrap and also for the axial movement of the rotor.

The instruments used were Wayne-Kerr DM 100 Displacement Meters and the probes were calibrated by means of precision gauge blocks and an accurately ground cylinder of diameter equal to that of the journal. The gap width at the midpoints of several regions of wrap could be obtained directly by connecting the outputs of two parallel probes, one monitoring the displacement of the foil and the other that of the journal, to the terminals of a differential amplifier.

It is estimated that the amplitudes of motion of the rotor, based on the average sensitivity-scales appended to various oscillograms, involve maximum possible errors the order of 5%. This estimate includes variations of sensitivity between individual probes and the variation in sensitivity due to nonlinearity of probe outputs at relatively large probe offsets. The corresponding accuracy of scales in oscillograms of gap width is estimated to be within 10%. The frequency response of the displacement meters, inclusive of output filters, was flat to at least 2.5 kc and quite adequate in the range of experimental speeds of rotation and frequencies of excitation.

The speed of rotation was measured by means of an optical probe and an MTI KD-38 Fotonic Sensor, using a Hewlett-Packard

Model 523B Electronic Counter. Above 100 RPS, the speed could be measured and maintained with an accuracy better than 1%.

A digital-to-analog converter, integral with a Hewlett-Packard Model 560A Digital Recorder, was used in conjunction with a Model 523B Electronic Counter to obtain a d.c. signal proportional to the rotor speed.* This signal, applied to the horizontal plates of an oscilloscope, permitted direct photographic recording of the rotor amplitude-response and of foil clearance as functions of the rotational speed. It is estimated that the accuracy with which the rotational speed can be determined in the oscillograms of scans of the rotor amplitude-response and of the gap width is of the order 15 RPS, the error being due mainly to slow drift of the converter output. The recorder furnished automatically printed data of the variation of the rotational speed during coastdown, from which frictional losses could be calculated.

The vibrator (MB, Model C-10 Exciter) was capable of transmitting a force of 1200 lb within a frequency range 5 - 3000 CPS. Maximum displacement amplitudes of 0.5 inches and velocities of 70 in/sec could be realized. The accelerometers were Endevco, crystal type, used in conjunction with Glemite amplifiers, having a flat response 5 cycles to 35 kc. Since high frequency, low amplitude components of excitation, such as multiples of the rotational speed related to the number of nozzles, orifices, or turbine buckets, and other spurious high frequency disturbances could be sensed by the accelerometers, the amplified outputs of the latter were passed through SKL variable bandwidth filters to eliminate frequency components higher than 1500 CPS. This arrangement permitted proper control of motion of the vibrator by the in-line accelerometer and in a nearly sinusoidal vibration input to the rotor-support assembly, except at a number of isolated structural and foil-rotor resonances.

*Speed manually controlled.

EXPERIMENTS

Rotation in the Horizontal Attitude and Response to Residual Imbalance

The first series of experiments was conducted with the rotor in the horizontal attitude. A preload tension $T_0 = 2.0$ lb/in was applied to the 0.001 inch thick, 1.5 inch wide molybdenum foils. The foil-lift supply pressure was $p_\ell = 30$ psig. Upon removal of counterbalance weights, the rotor displaced downward by approximately 0.002 inch, returning to a position approximately 0.0003 inch below the reference axis when the foil bearings were externally pressurized.

The bidirectional thrust bearing had a total axial clearance of 0.004 inch. In the pressurized mode of operation, the minimum clearance was 0.0014 inch because of dissymmetry produced by the thrust of the foil-lift supply pressure acting on the face seal. The minimum clearance was on the inboard side of the thrust bearing, in which the outer perimeter of the thrust pads coincided with the 3.25 inch diameter of the rotating end-disc, which served as a runner.

The test procedure followed in obtaining frequency scans of rotor response to remanent imbalance was to increase the speed very gradually (typically 2 - 3 RPS/sec, especially in the resonant bandwidth) and to accelerate in the pressurized mode to approximately 300 RPS. Following rapid cutoff of the foil-lift air supply and transition to the self-acting mode of operation, the rotor was accelerated to 750 RPS. After a few minutes of high-speed operation, during which speeds of 50,000 RPM were obtained on numerous occasions, the turbine air supply was discontinued and the rotor allowed to coast down, first in the self-acting mode to approximately 300 RPS, and thereafter in the pressurized mode.

A typical scan of response during acceleration is presented in Fig. 4. It can be seen that resonances occur in the pressurized mode only and that maximum amplitudes occur in a narrow bandwidth, centered at approximately 140 RPS. The resonant orbits, corresponding to maximum x- and y-amplitudes in the monitoring planes A and B that straddle each pair of foils, are shown in Fig. 5. The timebase displays in the same figure indicate that the motion was quasi-conical. The maximum amplitude at the midplane of bearing A was the order of 775 μ inches.

The variation of gap width with speed in the horizontal attitude, at one of the load-supporting foil segments, is illustrated in Fig. 6. At low speeds and in the pressurized mode of operation, the gap width was the order of 0.002 inch, increasing noticeably due to squeeze film effects in the region of resonance. The decrease of gap width, following transition to the self-acting mode at approximately 300 RPS, is quite drastic. The clearance is diminished by nearly an order of magnitude to approximately 250 μ inches, increasing to approximately 700 μ inches at 600 RPS, and to 900 μ inches at 750 RPS. On coastdown, the decrease of gap width with speed in the self-acting regime is moderated by additional slack, due possibly to thermal relaxation and following slippage of foil at the guides. During coastdown, just before re-pressurization, the clearance is approximately 700 μ inches, and thus appreciably wider than following transition to the self-acting mode during acceleration of the rotor.

Response to Symmetric and Asymmetric Imbalance in the Horizontal Attitude

The remanent imbalance of the rotor, referred to the midplanes of the end discs (approximately 15 inches apart) was 350 μ in-oz in each plane.* As noted in the preceding section, the maximum amplitude of response to remanent imbalance in the midplane of bearing A was approximately 775 μ inches and occurred at a rotational speed of very nearly 140 RPS (Fig. 5).

*The directions of remanent imbalances in each balancing plane could not be accurately determined. The magnitude of the imbalance vector can be determined with a much greater degree of certainty than its angular position.

Various amounts of symmetric and asymmetric imbalance were then introduced in the form of screws, in the midplanes of the end discs. The screws were of equal weight and the distances of their mass centers from the rotor axis were known within 2%.

A comparison is made in Fig. 7 between maximum, or near-maximum, amplitudes at three levels of symmetric and asymmetric imbalance. The oscillograms of rotor orbits in the midplanes of bearing A and bearing B correspond to imbalances of 1,510 μ in-oz, 6,050 μ in-oz and 31,400 μ in-oz in each plane. These levels correspond respectively to 4.4, 17.4 and 90.0 times the amount of remanent imbalance. The orbits in Fig. 7 were recorded in the pressurized mode at 140 RPS (resonance), and in the self-acting mode at 600 RPS (rated speed).

It can be seen that the maximum amplitudes* associated with highest level of symmetric and asymmetric imbalance were the order of 0.0013 inch to 0.0015 inch. At 600 RPS, in the self-acting mode of operation, the rotor amplitudes in the bearing midplanes remained below 250 μ inches at the highest level of imbalance.

It is instructive to note at this point the difference between the gap width in a foil bearing and the clearance of a rigid-surface bearing. In the latter case, a 3 mil diameter orbit could hardly be accommodated within the clearance circle of a representative gas bearing. In the case of the foil bearing, both foil and journal can displace, without diminishing the clearance to dangerously small proportion. Should contact occur briefly, the distribution of load over the effective area of wrap of a flexible and conforming foil results in far less destruction than the concentrated loading due to impact and rubbing in a rigid-surface bearing.

During the first run in the vertical attitude, the experimenters inadvertently omitted to remove the screws corresponding to the highest level of asymmetric imbalance and were consequently puzzled by relatively large orbits. The screws were removed and the experiments were

*To be interpreted as one-half of the maximum orbit dimension.

not repeated in the vertical attitude, since the effect of imbalance in the presence of gravity load, in the horizontal attitude, represents a more adverse condition.

Rotation in the Vertical Attitude and Response to Residual Imbalance

It is well known that conventional, fluid-film journal bearings, and gas bearings in particular, are plagued by the phenomenon of self-excited vibrations of rotors, frequently referred to in the literature as "half-frequency whirl," and more appropriately as "fractional-frequency whirl." This type of instability is particularly prone to occur with high-speed rotors operated in the concentric position, that is, in the absence of radial loading. The threshold speed of instability is very sensitive to the rotor mass, an increase of the latter having a very unstabilizing effect.

In the course of an experimental study of foil bearings, which preceded the present investigation [5,6], no whirl instability was encountered with 1.0 lb and 2.4 lb rotors in either the horizontal or vertical attitudes and at speeds of 60,000 RPM. Results of the present investigation showed the operation of a 20.9 lb rotor* to be stable in both the vertical and horizontal attitudes at speeds up to 50,000 RPM, wherein the speed limit was dictated by the strength of interference fits of journal sleeves on the rotor, and not by imminent danger of instability.

The test procedure for runs in the vertical attitude was essentially identical with that described in the preceding section. A typical scan of response to remanent imbalance during coastdown is presented in Fig. 8. The maximum x and y amplitudes in the monitoring planes A and B occurred in the pressurized mode, in a narrow frequency bandwidth centered approximately at 140 RPS, which was nearly coincident with the resonant bandwidth observed in the horizontal attitude. The orbits corresponding to these maxima are shown in Fig. 9, in conjunction

*Based on unit projected bearing area, the masses of the three rotors referred to in the foregoing are in the ratio 1.0:2.4:2.8.

with timebase displays of the x-probes. The latter are indicative of the motion of the rotor axis and the extent to which it is quasi-conical or quasi-cylindrical.*

Because of symmetry and approximately isoelastic properties of the foil-bearing supports, and because of the rotor mass distribution with respect to bearing location, the resonances corresponding to 4 degrees of freedom occur in a narrow frequency band and the peak amplitudes of all modes coalesce. These resonances are in the pressurized mode of operation and it is evident that the resonant bandwidth of the self-acting mode lies well below the transition speed of 300 RPS.

It can be noted that scans of amplitudes of response in the low speed range displays a series of rather well defined peaks, at definite speeds of rotation. While the orbits which characterize the maximum rotor excursions are synchronous, the orbits corresponding to the minor peaks are multi-looped, and the number of loops increases with decreasing speed. The relevant timebase displays show corresponding ultraharmonics superposed on the synchronous motion. This phenomenon of ultraharmonic resonances in the pressurized mode of operation was observed and has previously been described in references [5] and [6]. It was shown that the speed at which an ultraharmonic resonance occurred, when multiplied by the ultraharmonic number (ratio of orbital to the rotational frequency), was nearly equal to a speed of synchronous resonance. A series of orbits in the frequency bandwidth of the first ultraharmonic resonance is illustrated in Fig. 10, together with corresponding timebase displays of the x-probes. Clearly, the rotor axis describes two revolutions for each revolution of the rotor about the axis. The reader will note that the average of the four speeds in Fig. 10 is approximately 67 RPS. Referring to Fig. 9, and taking the average of the four speeds, 138 RPS, as the speed of synchronous resonance, it will be noted that the latter occurs at very nearly twice the speed of the first ultraharmonic resonance.

*The literature dealing with the motion of rotors in bearings abounds with references to "circular and elliptical" orbits and "cylindrical and conical" motions of the rotor axes. These simplified descriptions are convenient, but paths described by points on the rotor axis and surfaces traced by the axis itself are of far more complex geometry.

A scan of the gap width at foil sector B_{13} , adjacent to the foil lock, is shown in Fig. 11. This scan can be compared with the oscillogram presented in Fig. 6, which corresponds to the same foil sector when radially loaded (horizontal attitude). In general, the gap widths appear to be of the same order of magnitude. During acceleration in the vertical attitude, the clearance immediately after transition to the self-acting mode was larger than in the horizontal attitude. Thereafter, the increase of gap width with speed in the horizontal attitude appears to have been greater than the increase in the vertical attitude. At 750 RPS. the gap widths in both attitudes were nearly equal.

The scans of gap width in the pressurized mode of operation display a relative maximum in the resonant frequency bandwidth, and this is attributed to an increase of the time-average pressure in the gap due to squeeze-film effects. In the pressurized mode of operation the measured gap widths at the foil sector B_{13} , in both the horizontal and vertical attitudes, were the order of 0.002 inch. At 300 RPS, in the self-acting mode, the clearances were the order 250 to 750 μ inches, increasing to approximately 900 μ inches at 750 RPS. It appears that gravity loading in the horizontal attitude is compensated largely by unloading of the upper foil sectors.

Comparison of gap widths at other foil sectors indicated variations of approximately 20%, but it must be emphasized that gap measurements were considered to be accurate to within 10% only. The reader is also alerted to the fact that the gap width decreases with tension and that relatively small extensions δl , comparable in magnitude with the gap width h^* , result in very appreciable increments of tension δT .[†] These differences and asymmetries are almost unavoidable in any realistic application. The encouraging fact is that the operational characteristics of the foil-bearing supported rotor seemed to be quite insensitive to these inherent nonuniformities, as evidenced by the successful operation of the simulator in both the vertical and horizontal attitudes.

[†] Note that, approximately $h^* \sim T^{2/3}$ and $\delta T/\delta l = Et/l \sim 10^4$.

Two coastdown curves from a speed of 750 RPS are plotted in Fig. 12. Although these plots correspond to operation in the vertical and in the horizontal attitudes, it can be seen that the curves are nearly congruent, indicating that frictional losses were nearly identical. The total frictional power loss at rated speed of 36,000 RPM, inclusive of windage, foil bearing and thrust bearing losses, was approximately 0.78 kw. An estimate, based on the assumption of simple Couette flow and an average gap width of 800 μ inches, with air as a lubricant, shows the foil-bearing loss to be the order of 0.22 kw.

Response to Unidirectional Excitation by a Vibrator (Shake-Table)

The experiments pertinent to the response of the system to rotating imbalance furnished no information with respect to resonances in the self-acting mode. These resonances, since they occur in a frequency interval adjacent to the resonant bandwidth in the pressurized mode and below the transition speed to the self-acting mode, could not be consequently observed in the course of previous experiments.

The purpose of the shake-table experiments was to determine various performance characteristics of the rotor when subjected to periodic unidirectional excitation. A view of the foil-bearing supporting rotor, mounted on an oil-floated plate attached to the exciter head, is shown in Fig. 13. The excitation was imparted along a line perpendicular to both the rotor axis and the direction of gravity, that is perpendicular to the bisector of the unloaded foil segment.* The tests were conducted at the rated speed $N = 36,000$ RPM and the rotor was supported on 1 mil molybdenum foils, preloaded to approximately 2.0 lb/in.

Scans of response with increasing and decreasing frequency of excitation, in the range $25 < f_e < 1000$ CPS, are illustrated in the oscillograms of Fig. 14. Shown also are outputs of three accelerometers, the

*In a set of similar experiments described in references [5] and [6], the direction of gravity coincided with the axis of rotation and excitation was along a bisector passing through the foil lock.

locations of which are indicated in the accompanying schematic diagram of the shake-table and the foil rotor system.* The scans are similar and show that resonances occurred in the narrow bandwidth centered approximately at $f_e \approx 185$ CPS. The maximum in-line excursions corresponding to an excitation level $G_x \approx 0.8$ (peak amplitude) were $(x_A)_{\max} \approx 2100 \mu\text{in}$ and $(x_B)_{\max} \approx 1250 \mu\text{in}$. The orbits corresponding to these maximum excursions are shown in Fig. 15 and the frequencies of excitation at which these maxima occurred were 170 CPS and 200 CPS respectively. The motion in the resonant region was quasi-cylindrical, so that the traces of the in-line probe outputs in the second oscillogram of Fig. 15 are nearly in-phase and do not differ greatly in amplitude.

The motion of the rotor in the monitoring plane A, at various frequencies of excitation, is illustrated in Fig. 16. The reader will note that the displacement was nearly collinear with the excitation, changing into a narrow quasi-elliptical orbit at resonance. The time-base oscillogram in Fig. 16 shows the phase shift between in-line acceleration and in-line displacement in passing through resonance. The overall collinearity of excitation and displacement can also be noted in the first oscillogram of Fig. 17. The latter shows that at $N = 600$ RPS and $f_e = 300$ CPS, the amplitude of motion increases nearly linearly at a rate of approximately $175 \mu\text{in/g}$ in the range of excitation $1 g \leq G_x \leq 5 g$. The second oscillogram shows the sinusoidal waveforms of the G_x accelerometer output. We note in passing that, unlike in other types of fluid-film bearings, excitation at $f_e = N/2$ causes no loss of load capacity and an associated growth of amplitude of motion.

* G_x was the controlling accelerometer, with the output of G'_x and G_y used to assess yawing and pitching of the vibrating support-plate.^y The plate was floated on a thin film of oil, on a granite table, and was bolted to the exciter head. No other constraints were furnished. The plate translated parallel to itself up to approximately 400 CPS. Thereafter, various structural resonances occurred and the motion was more complex.

CONCLUSIONS

The experimental results presented in the preceding sections pertain to a 21-pound rotor, supported by foil bearings and operated stably in both the vertical and horizontal attitudes at speeds up to 50,000 RPM. The mass, the polar and transverse moments of inertia, the bearing span and the bearing stiffness of the simulator matched closely those of a Brayton Cycle Turbo-Alternator undergoing development under the sponsorship of NASA [7].

Of the advantages of foil bearings listed below, all have been substantiated by extensive tests in the course of the present and preceding studies:

- a) Freedom from self-excited vibrations, commonly referred to in literature as "half-frequency" or "fractional-frequency" whirl. This consideration is particularly important in the state of weightlessness, in which instability of gas-bearing supported rotors is most likely to occur [8, 9, 10].
- b) Excitation at frequency equal to half the speed of rotation causes no loss of load capacity. The half-speed danger point characterizes most rigid, fluid-film bearings, but is absent in foil bearings [11].
- c) Motion of the journal is not constrained by the narrow confines of the clearance circle. Both foil and journal can displace while maintaining the lubricating film. Rotor excursions several times the order of clearance of a conventional gas bearing can thus be accommodated.
- d) The foil bearing is extremely forgiving of foreign particles. It accommodates geometrical imperfections and misalignments. Manufacture is simple and no stringent requirements exist with regard to dimensional accuracy and roundness. The performance of foil bearings appears to be quite insensitive

to large variations of various bearing parameters and operation can be maintained under conditions which could not be tolerated with other types of bearings.

At the present state of this relatively new bearing art, possible disadvantages of foil bearings, in comparison with other types of bearings, may be the following:

- a) Relatively low stiffness (typically 15,000 lb/in for a 2.5-inch diameter, 1.5-inch long bearing).
- b) Relatively greater journal-length requirement.
- c) More elaborate pressurization system for starting.

The foil bearing is not intended to compete in stiffness with other types of bearings, although an appreciable increase of stiffness can be achieved. The practicality of gas-lubricated foil bearings has been demonstrated as a method of support for high-speed turbomachinery. While incorporation of the present foil-bearing configuration in the overall design of turbomachines is in itself a practical proposition, further development is in progress. In order to capitalize fully on the potential of foil bearings, future development will be concentrated on problems related to improved and novel methods of foil mounting, reduction of journal length requirements, and simplification of starting methods. Concepts and devices to further the foregoing objectives are already under active consideration.

ACKNOWLEDGEMENTS

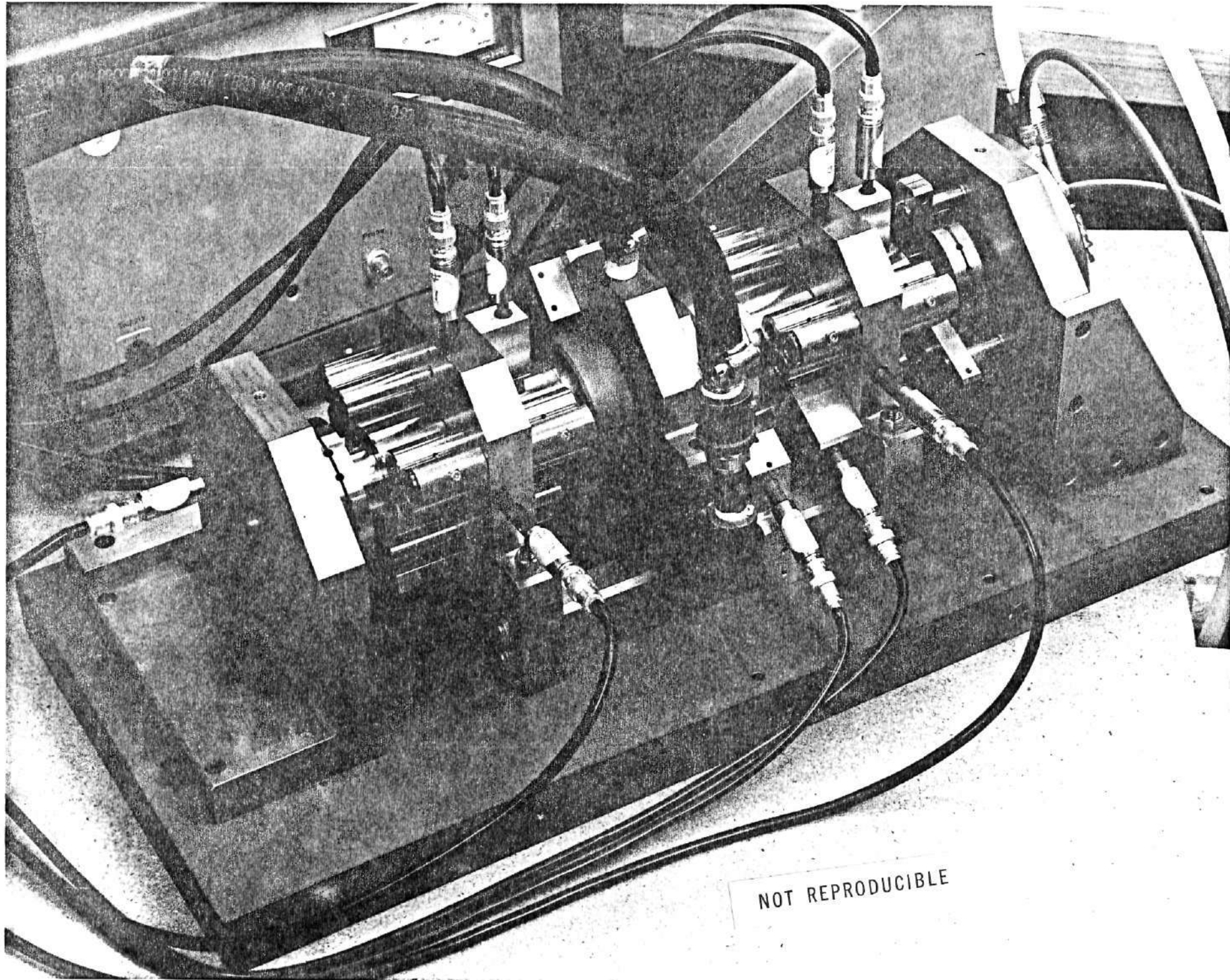
This research was sponsored by the National Aeronautics and Space Administration, Lewis Research Center, Cleveland, Ohio, under contract No. NAS3-11826. The author is indebted to Mr. William J. Anderson, Bearing Branch, Fluid Systems Component Division, NASA Lewis Research Center, for his cooperation and guidance with respect to technical objectives of this investigation.

Numerous discussions with Dr. A. Eshel and Mr. M. Wildmann, both of the Ampex Corporation, contributed significantly to the success of this study. The loyal support of Mr. B. Lawson and Mr. F. Schneider is gratefully acknowledged.

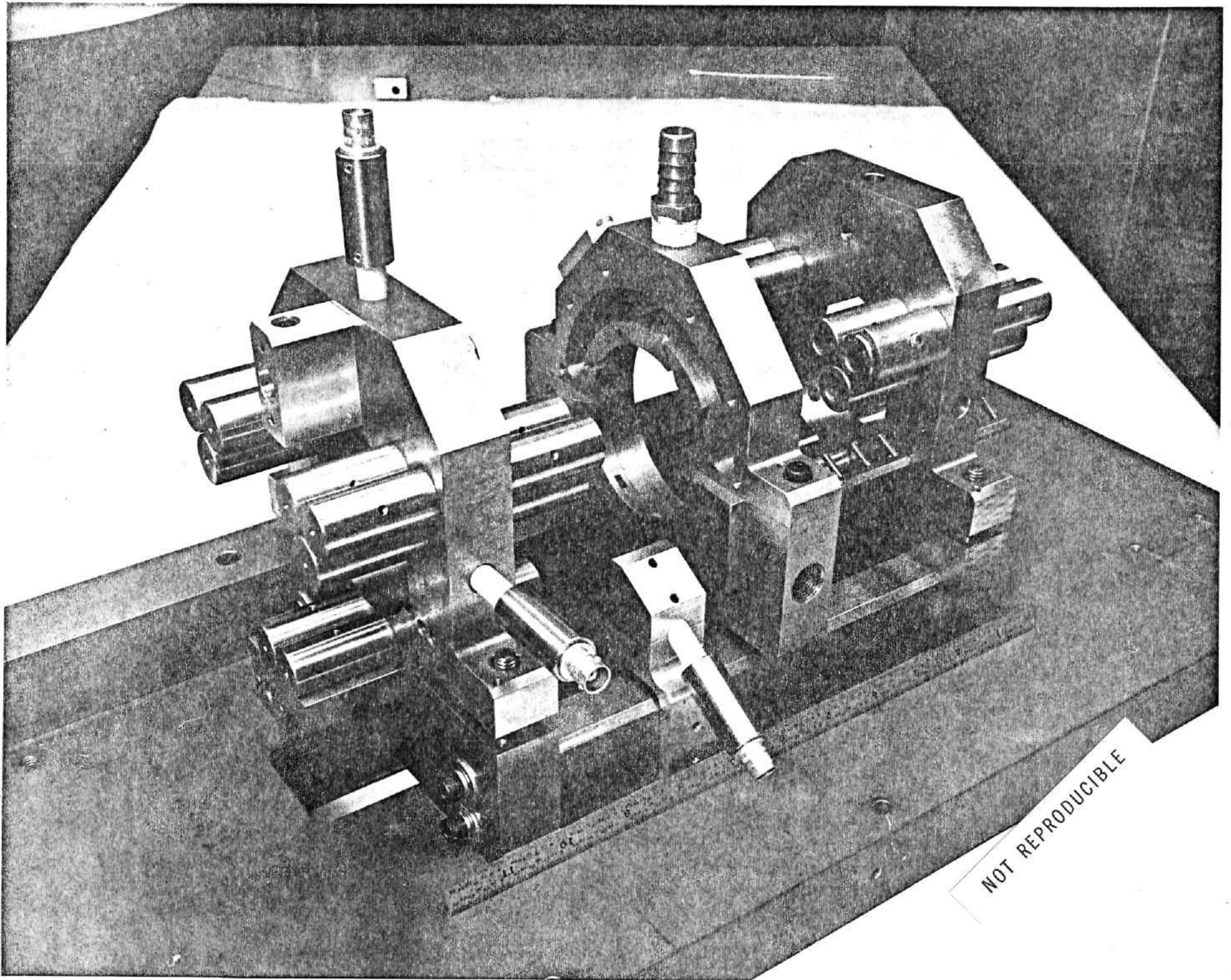
REFERENCES

1. L. Licht, "An Experimental Study of Elastohydrodynamic Lubrication of Foil Bearings," Part 1 - "Displacement in the Central Zone" and Part 2 - "Displacement in the Edge Zone," Journal of Lubrication Technology, Trans. ASME, Vol. 90, Ser. F, No. 1, January 1968, pp 199-220.
2. L. Licht, "An Experimental Study of Air-Lubricated Foils with Reference to Tape Transport in Magnetic Recording," Report No. 7, August 1966, Lubrication Research Laboratory, Columbia University, prepared under Contract Nonr-4259(14), Information Systems Branch and Fluid Dynamics Branch, Office of Naval Research, Washington, D.C.
3. G. K. Fisher, J. L. Cherubim and O. Decker, "Some Static and Dynamic Characteristics of High-Speed Shaft Systems Operating with Gas-Lubricated Bearings," Trans. of the First International Symposium on Gas-Lubricated Bearings, October 1959, ACR-49, Office of Naval Research, Washington, D.C., pp 383-410.
4. A. Stahler and A. Huckabay, "Analysis, Design, Fabrication and Testing of a Foil Bearing Rotor Support System," Ampex Corporation report RR 66-21, June 1966, prepared under Contract NASW 1221, NASA, Washington, D.C.
5. L. Licht, "An Experimental Study of High-Speed Rotors Supported by Air-Lubricated Foil Bearings," Part 1 - "Rotation in Pressurized and Self-Acting Foil Bearings" and Part 2 - "Response to Impact and to Periodic Excitation," Journal of Lubrication Technology, Trans. ASME, Vol. 91, Ser. F, No. 3, July 1969, pp 477-505.
6. L. Licht and A. Eshel, "Study, Fabrication and Testing of a Foil-Bearing Rotor Support System," NASA CR-1157, November 1968, prepared by the Ampex Corporation under Contract NASW-1456, NASA, Washington, D.C.
7. B. Sternlicht, "Gas-Bearing Turbomachinery," Journal of Lubrication Technology, Trans. ASME, vol. 90, Ser. F, No. 4, pp 665-679.
8. W. A. Gross, "Gas Film Lubrication," John Wiley and Sons, Inc. New York, 1962, pp 334-362.
9. C. H. T. Pan and B. Sternlicht, "Comparisons Between Theories and Experiments for the Threshold of Instability of Rigid Rotor in Self-Acting, Plain-Cylindrical Journal Bearings," Journal of Basic Engineering, Trans. ASME, Vol. 86, Ser. D, No. 2, June 1964, pp 321-327.

10. R. E. Cunningham, D. P. Fleming and W. J. Anderson, "Experimental Stability Studies of the Herringbone-Grooved, Gas-Lubricated Journal Bearing," Journal of Lubrication Technology, Trans. ASME, Vol. 91, Ser. F, No. 1, January 1969, pp 52-59.
11. J. S. Ausman, "On the Behavior of Gas-Lubricated Bearings Subjected to Sinusoidally Time-Varying Loads," Journal of Basic Engineering, Trans. ASME, Vol. 87, Ser. D, No. 3, September 1965, pp 589-603.



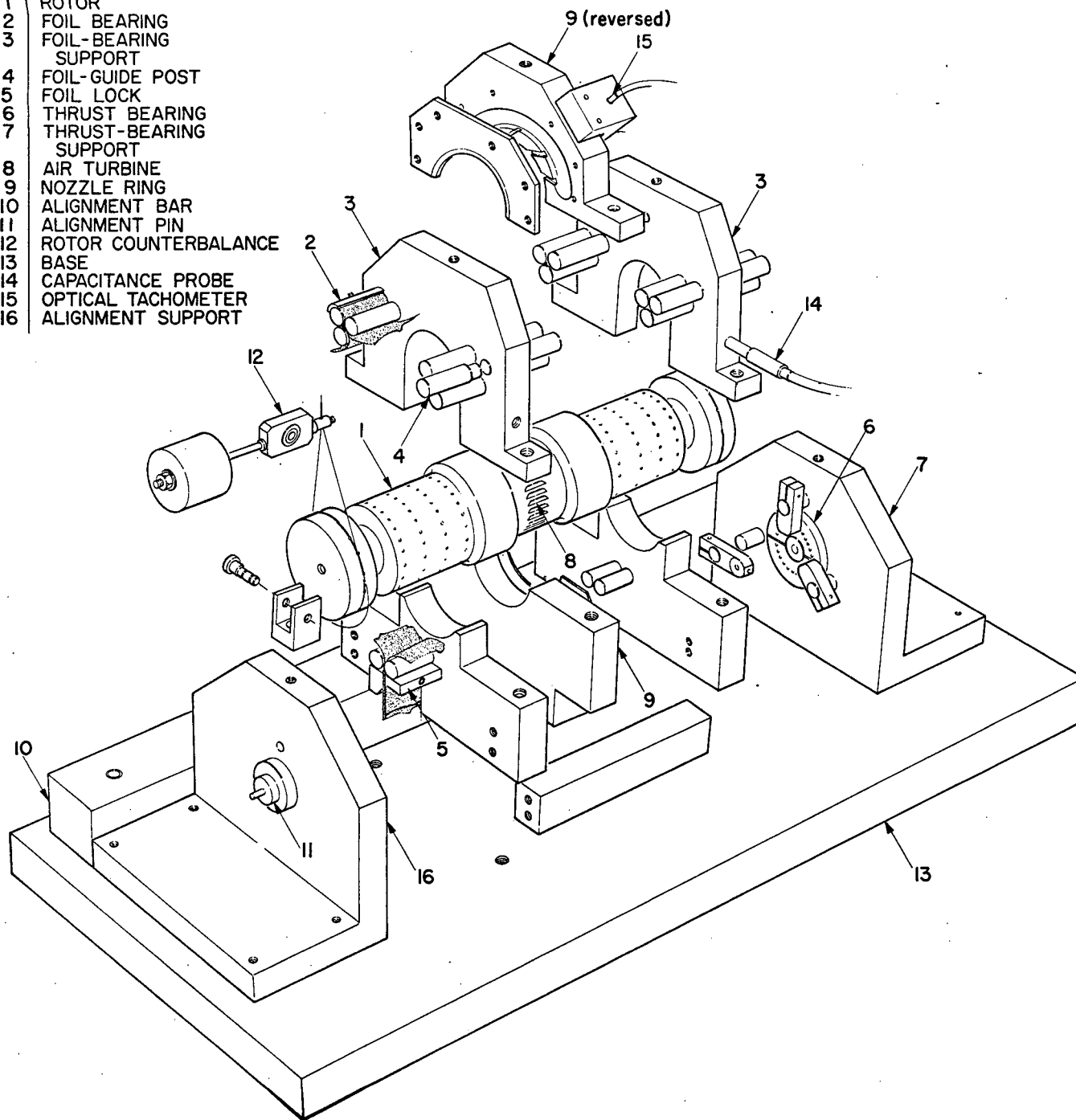
1. View of Foil-Bearing Supported Rotor in the Horizontal Attitude



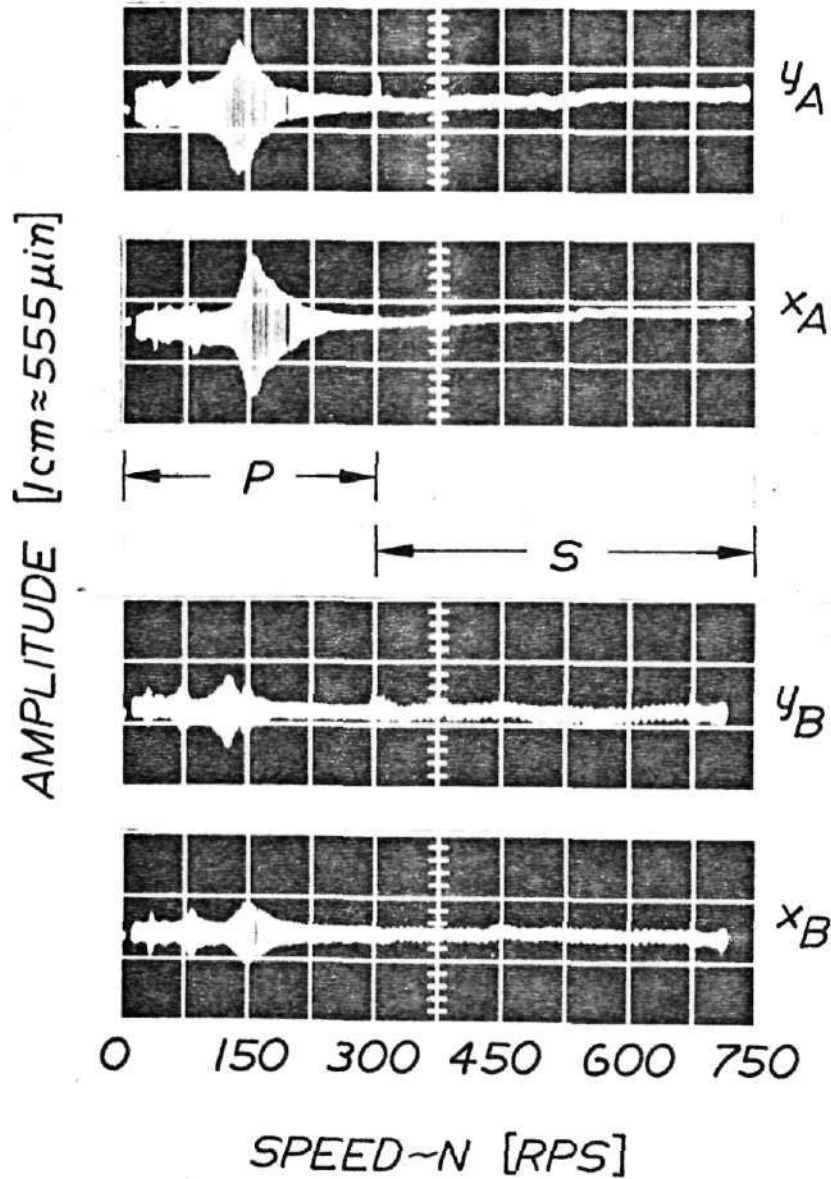
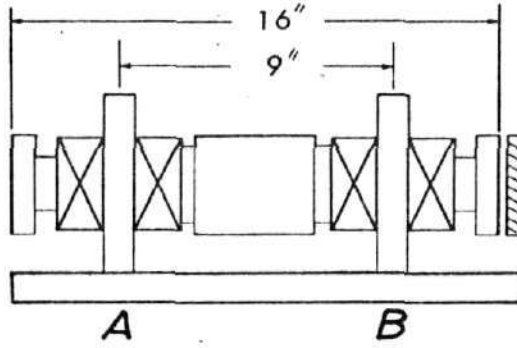
2. View of Foil-Bearing Support Assembly

LEGEND

- 1 ROTOR
- 2 FOIL BEARING
- 3 FOIL-BEARING SUPPORT
- 4 FOIL-GUIDE POST
- 5 FOIL LOCK
- 6 THRUST BEARING
- 7 THRUST-BEARING SUPPORT
- 8 AIR TURBINE
- 9 NOZZLE RING
- 10 ALIGNMENT BAR
- 11 ALIGNMENT PIN
- 12 ROTOR COUNTERBALANCE
- 13 BASE
- 14 CAPACITANCE PROBE
- 15 OPTICAL TACHOMETER
- 16 ALIGNMENT SUPPORT

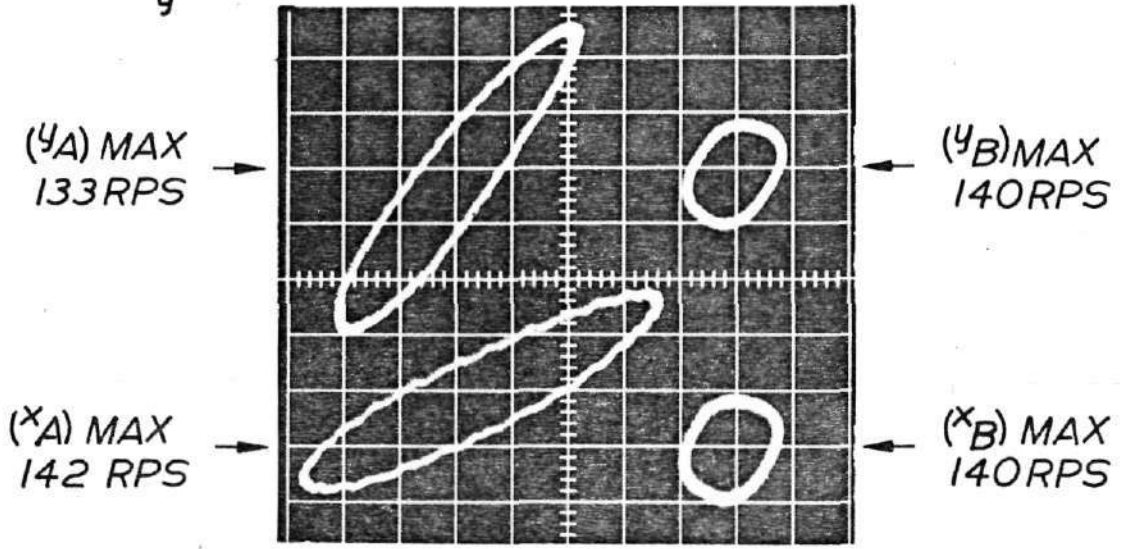
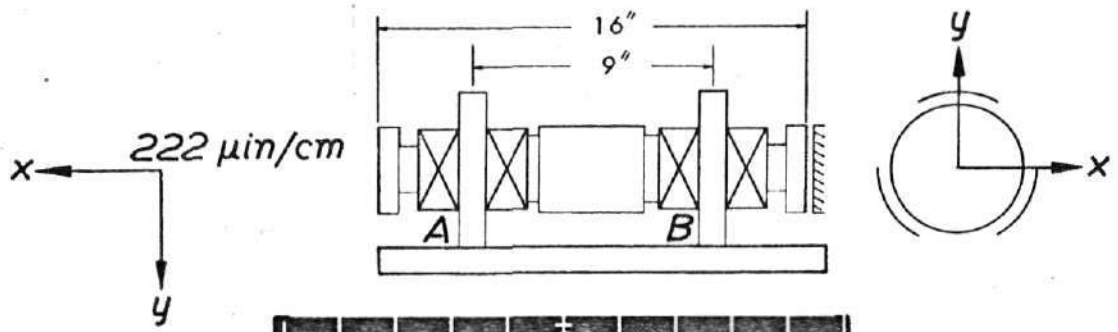


3. Schematic Diagram of Experimental Apparatus

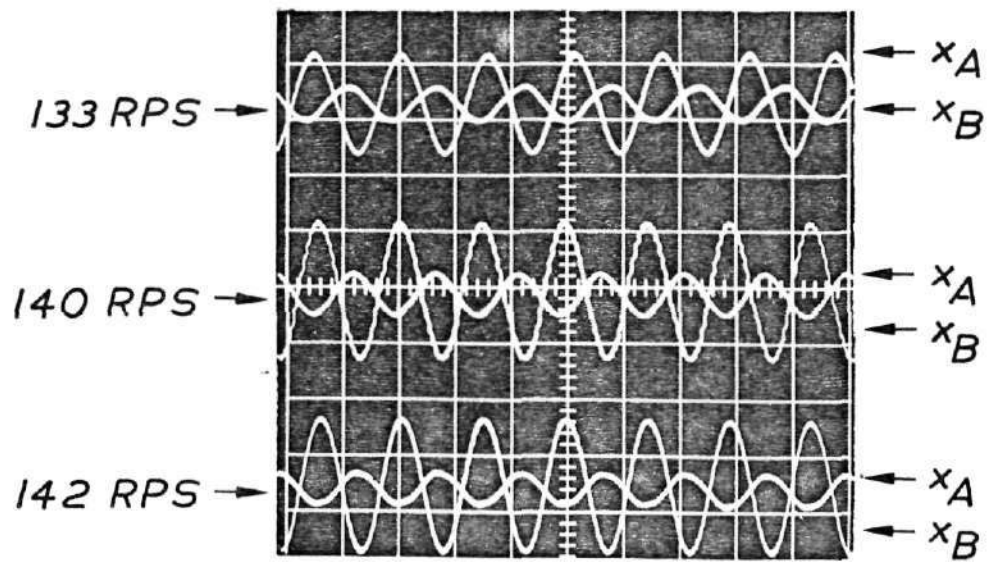


P =PRESSURIZED; S =SELF-ACTING

4. Scan of Response to Remanent Imbalance in Horizontal Attitude (Increasing Speed)

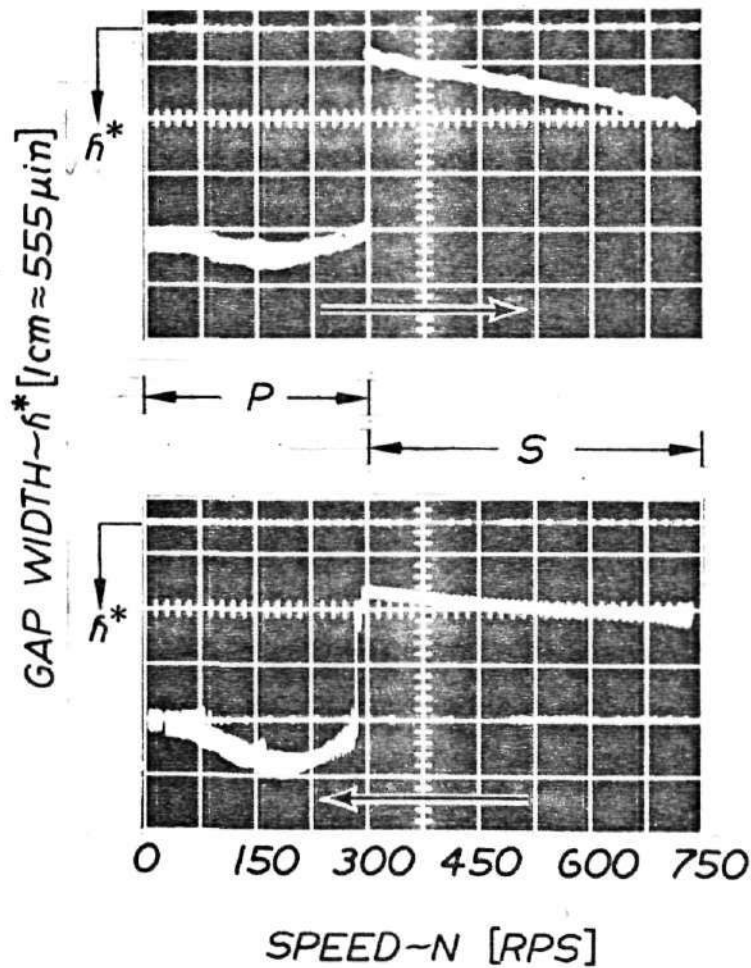
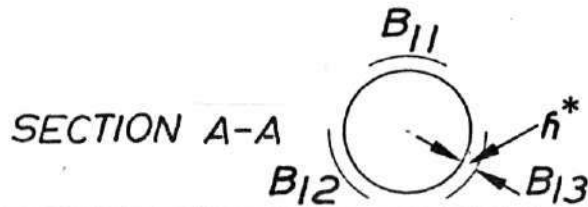
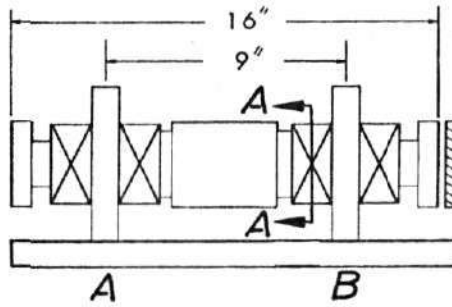


555 $\mu\text{in}/\text{cm}$; 5 ms/cm



NOT REPRODUCIBLE

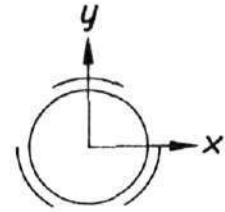
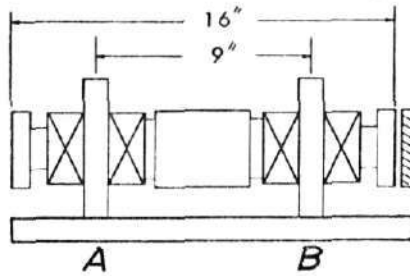
5. Rotor Orbits at Major Resonances (Horizontal Attitude - Pressurized Foil Bearing)



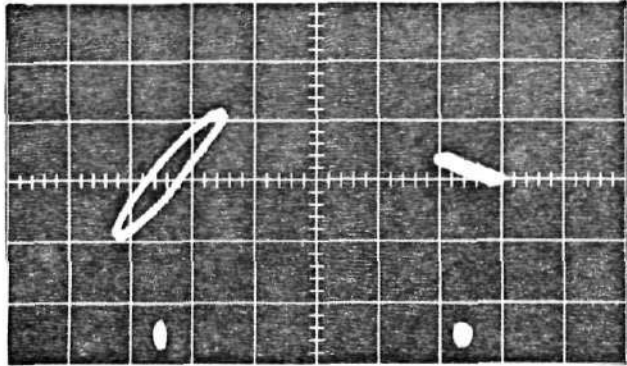
P =PRESSURIZED; S =SELF-ACTING

NOT REPRODUCIBLE

6. Variation of Gap Width with Increasing and Decreasing Speed in Pressurized and Self-Acting Modes (Horizontal Attitude - Foil Sector B_{13})

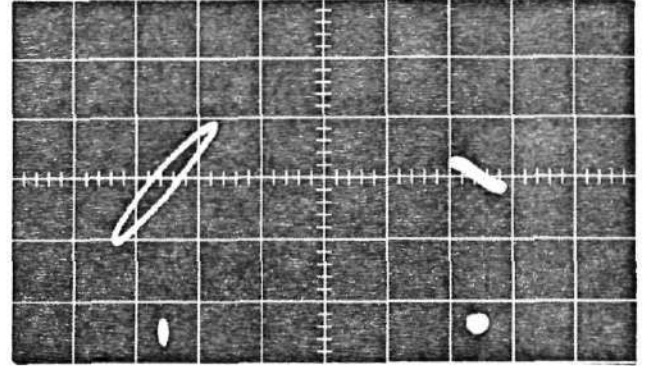


$\bar{u} = 1,510 \mu\text{in-oz}$



A

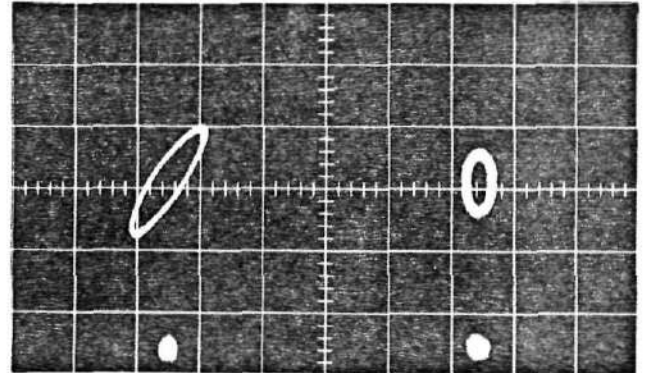
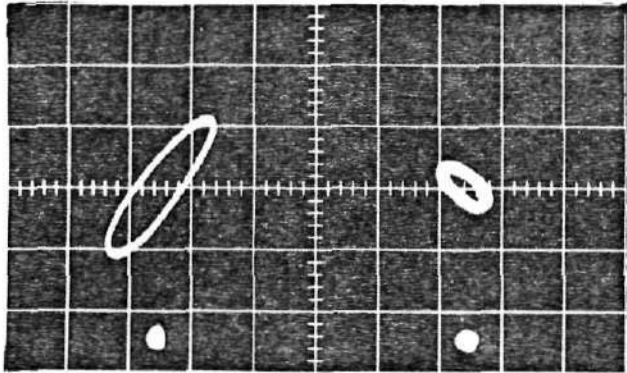
B



A

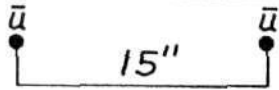
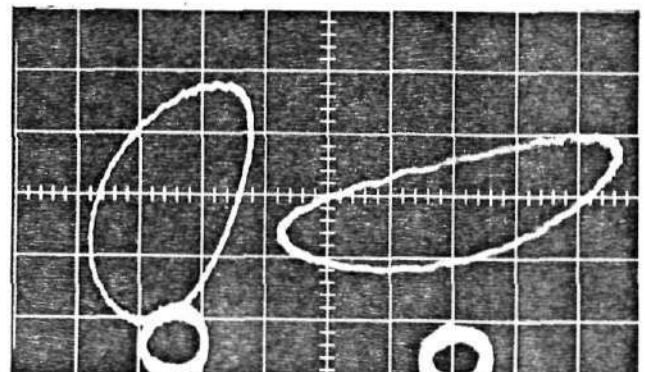
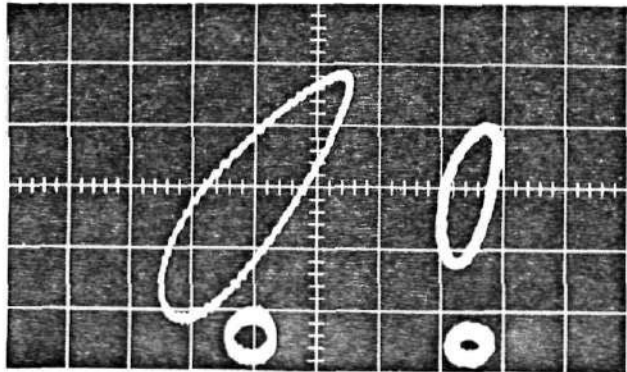
B

$\bar{u} = 6,050 \mu\text{in-oz}$

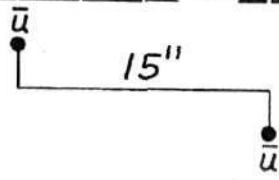


$555 \mu\text{in/cm}$

$\bar{u} = 31,400 \mu\text{in-oz}$

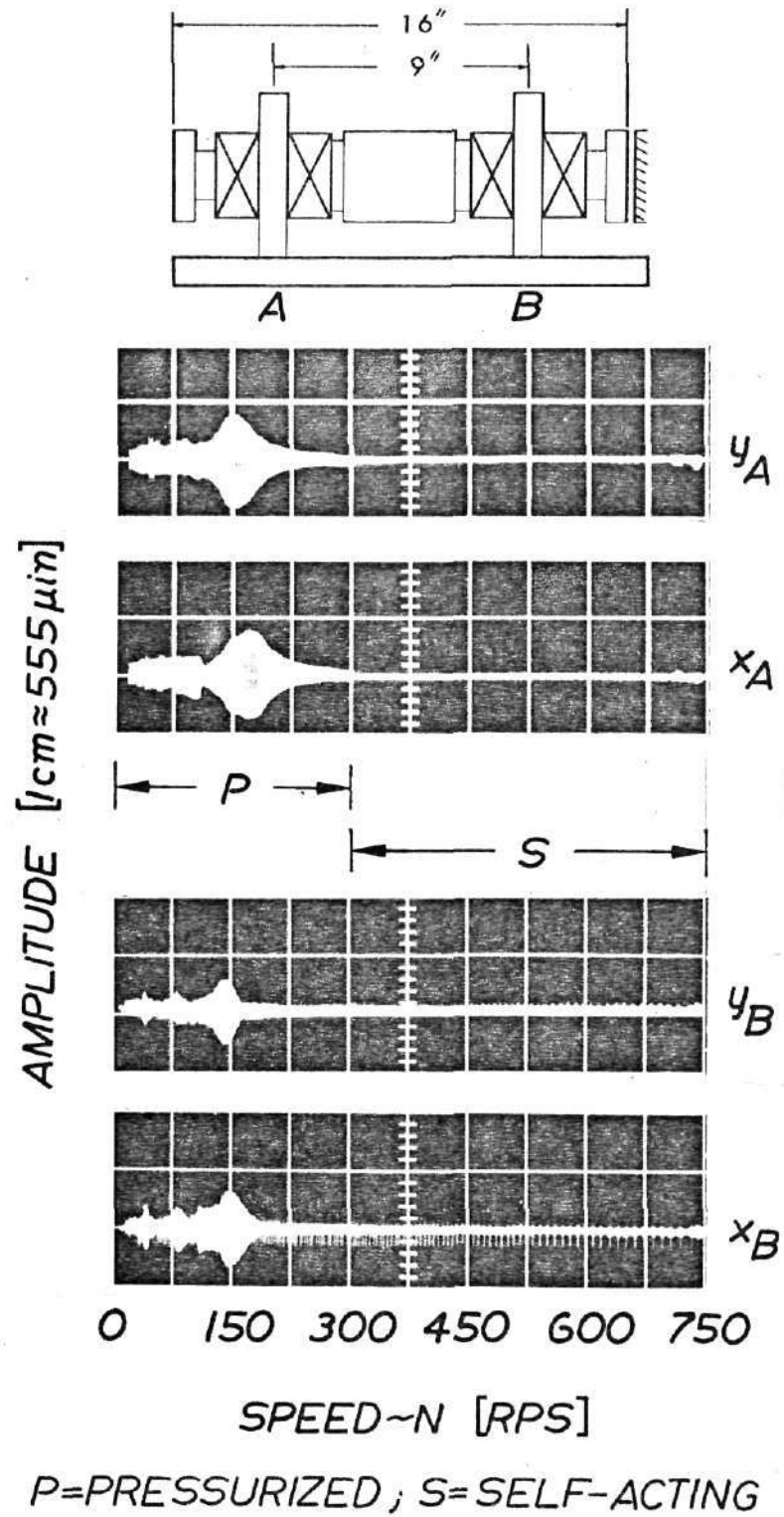


$555 \mu\text{in/cm}$



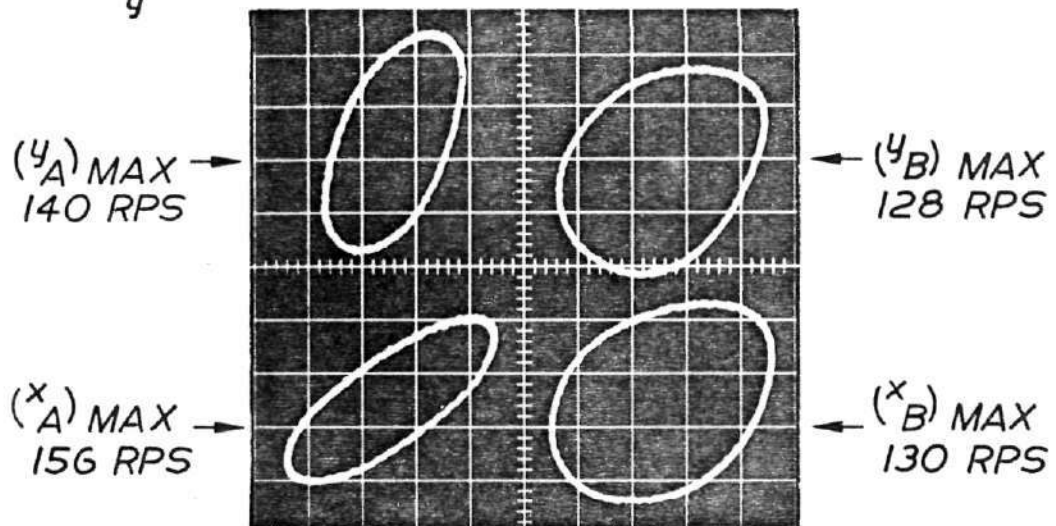
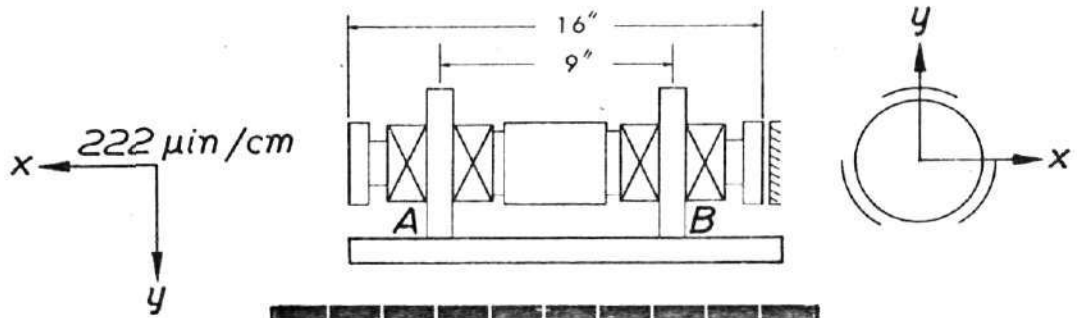
NOT REPRODUCIBLE

7. Comparison of Orbits in Horizontal Attitude at Various Levels of Rotating Imbalance (Upper Orbits at 8400 RPM ~ Resonant Bandwidth; Lower Orbits at 36,000 RPM ~ Rated Speed)

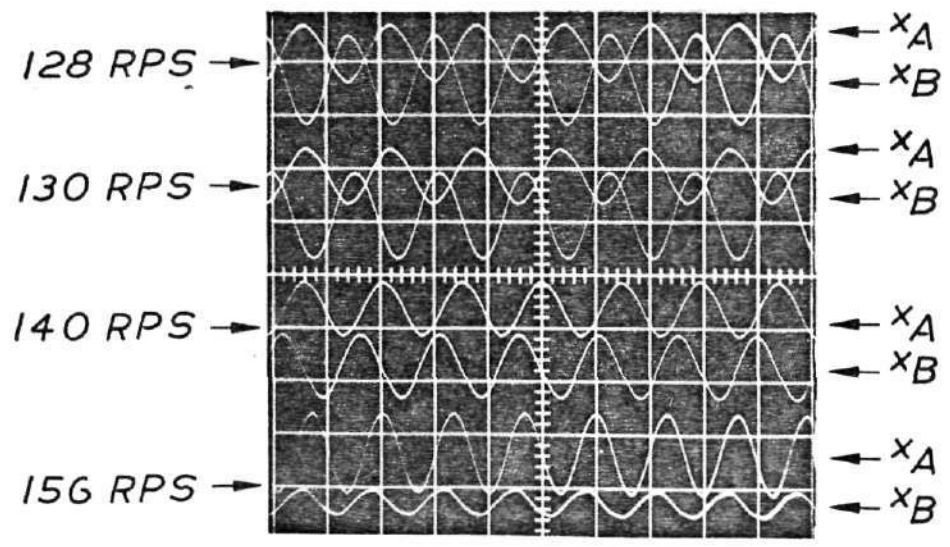


NOT REPRODUCIBLE

8. Scan of Response to Remanent Imbalance in Vertical Attitude
(Decreasing Speed)

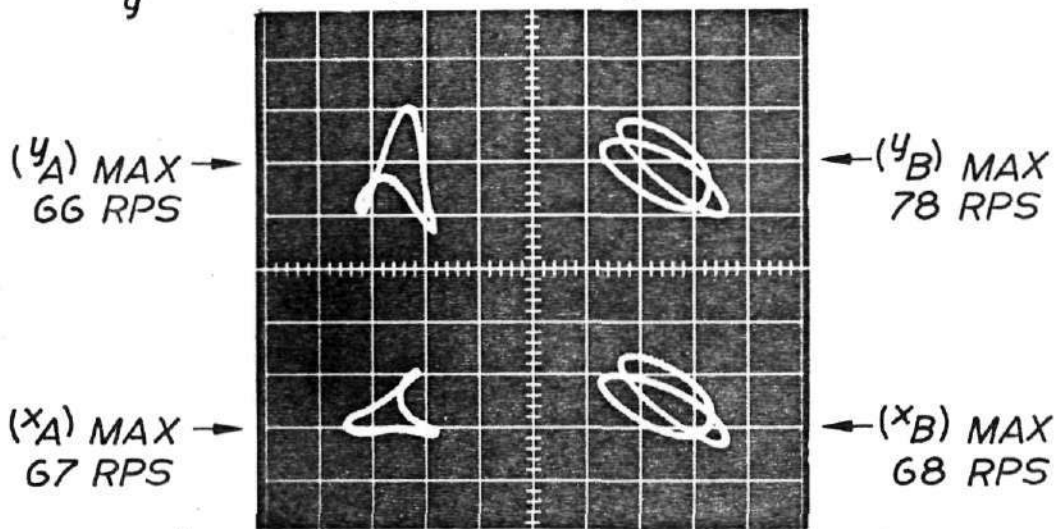
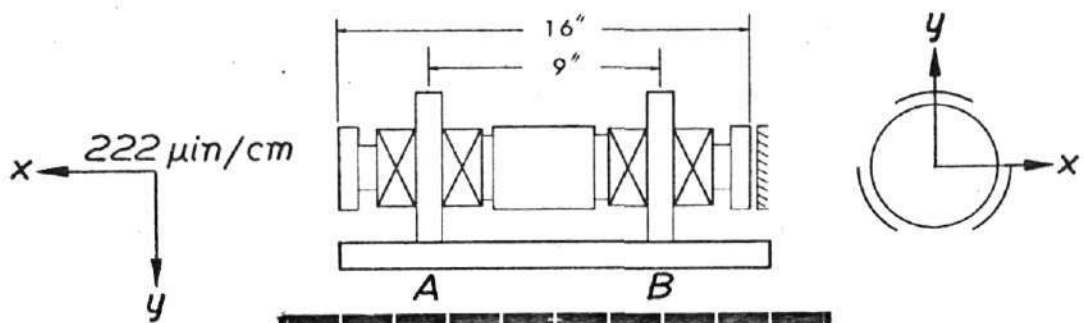


555 $\mu\text{in}/\text{cm}$; 5 ms/cm

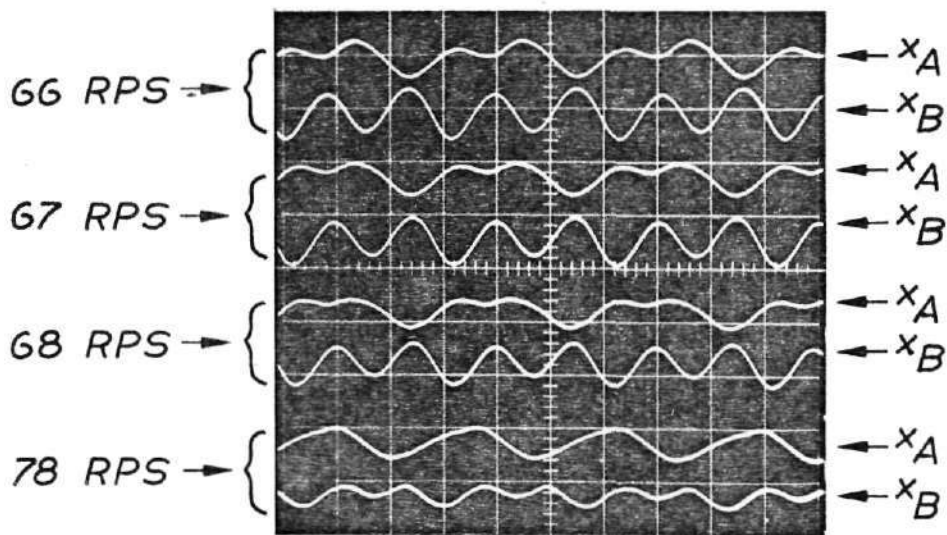


NOT REPRODUCIBLE

9. Rotor Orbits at Major Resonances (Vertical Attitude - Pressurized Foil Bearing)

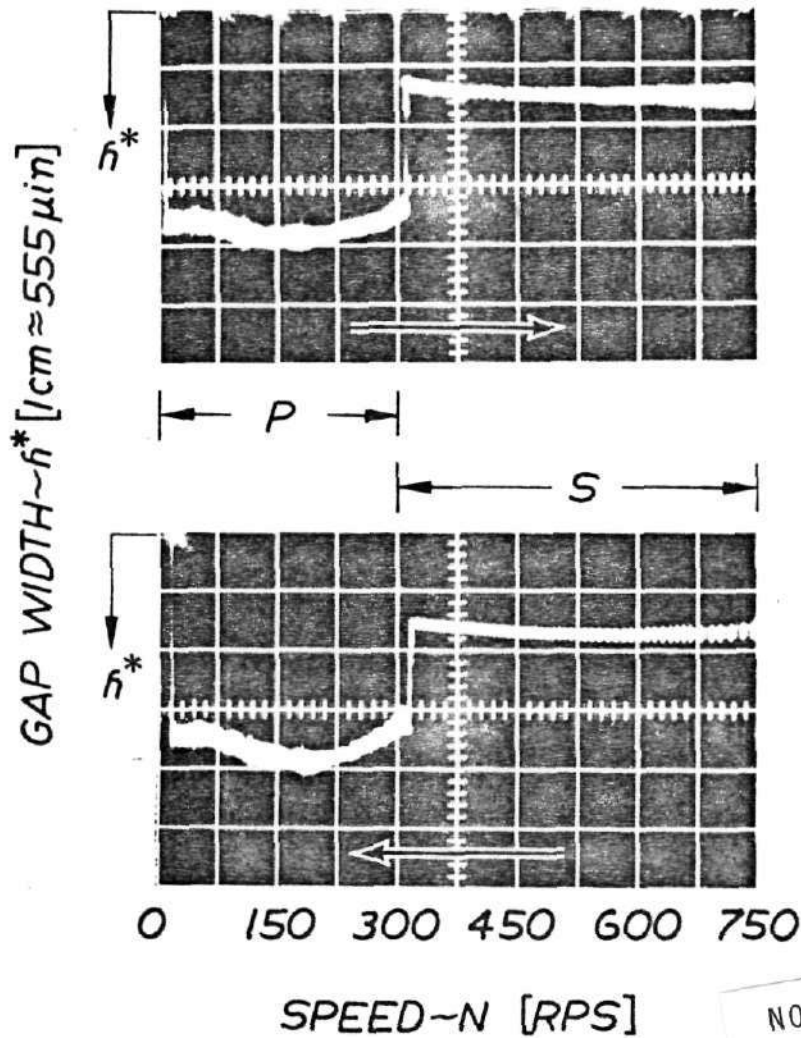
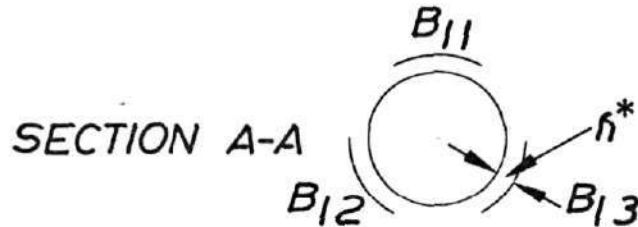
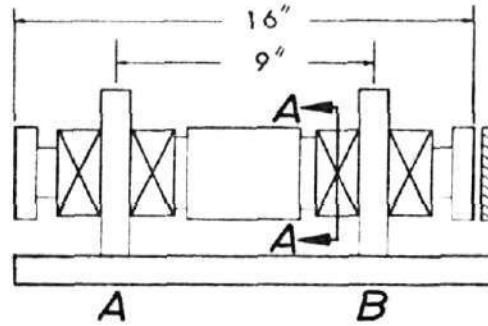


555 $\mu\text{in}/\text{cm}$; 5 ms/cm



NOT REPRODUCIBLE

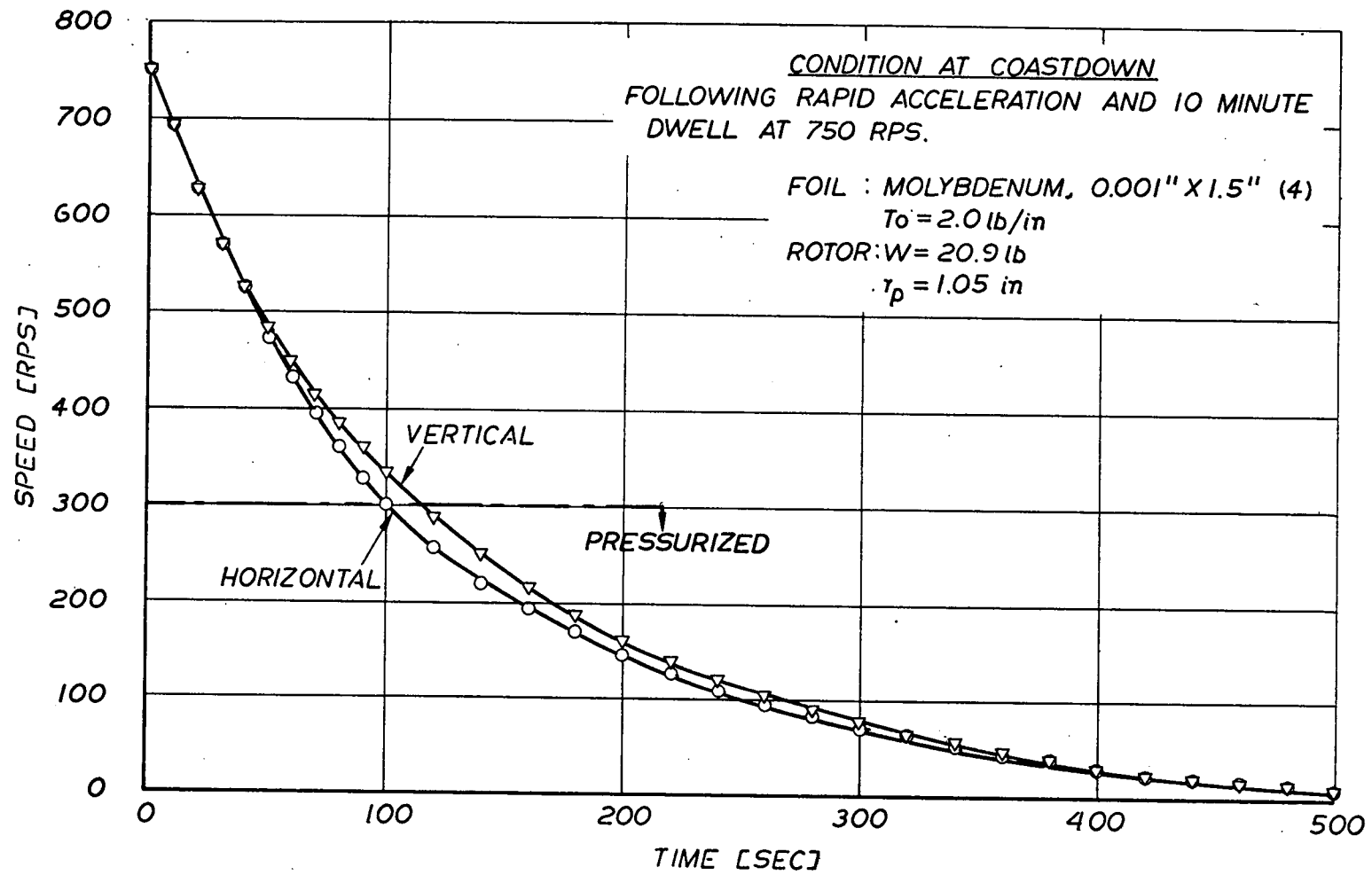
10. Rotor Orbits at First Overharmonic Resonances (Vertical Attitude - Pressurized Bearing)



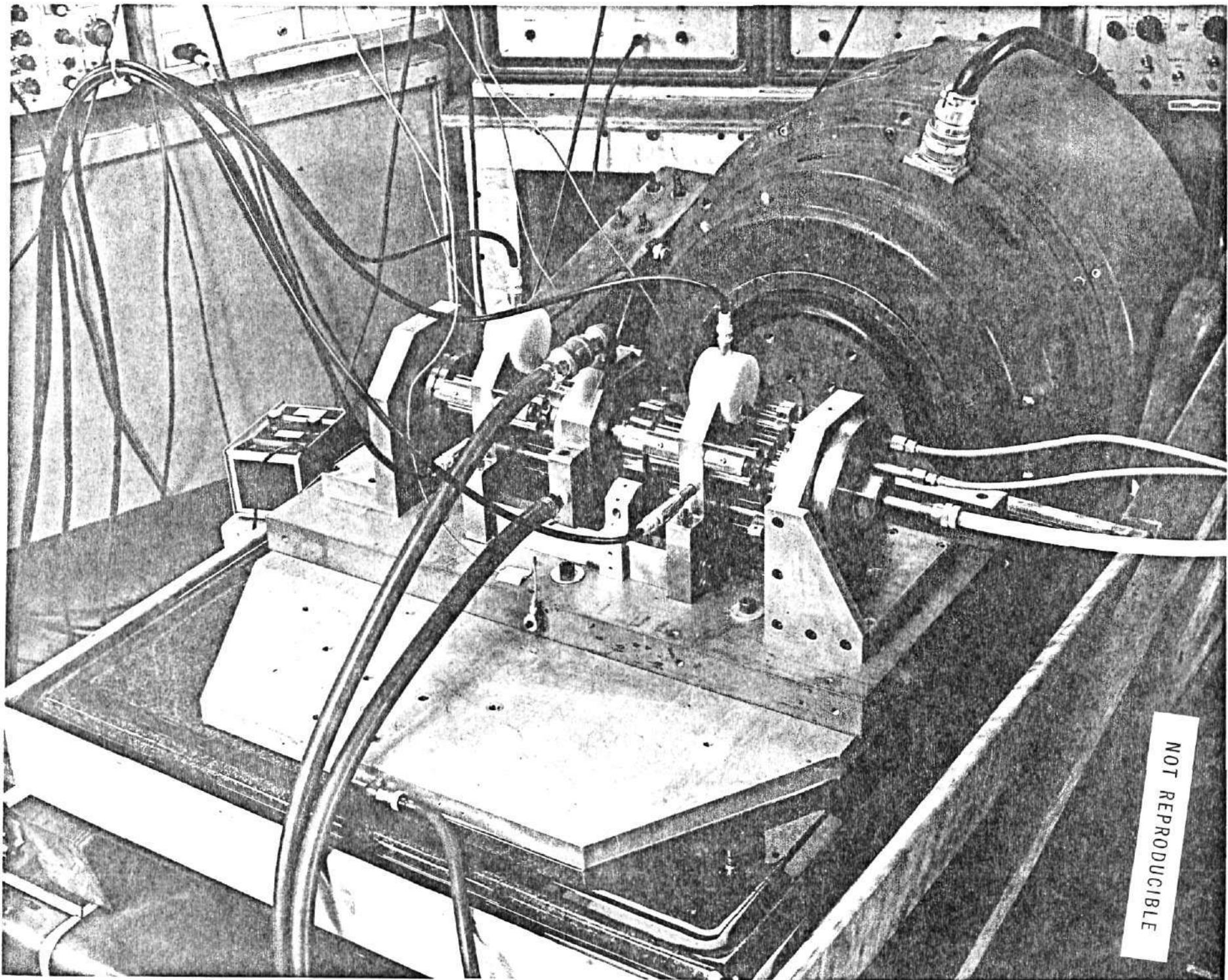
P=PRESSURIZED ; S=SELF-ACTING

NOT REPRODUCIBLE

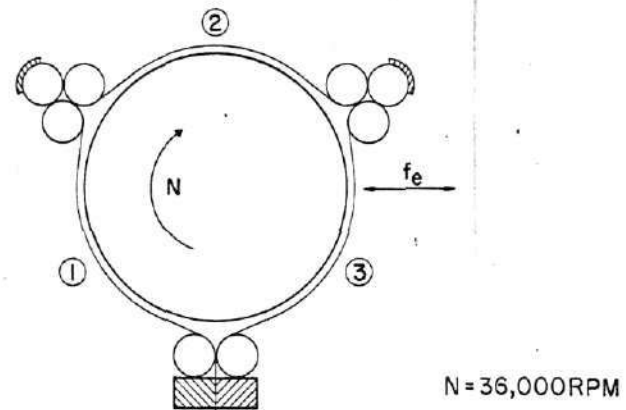
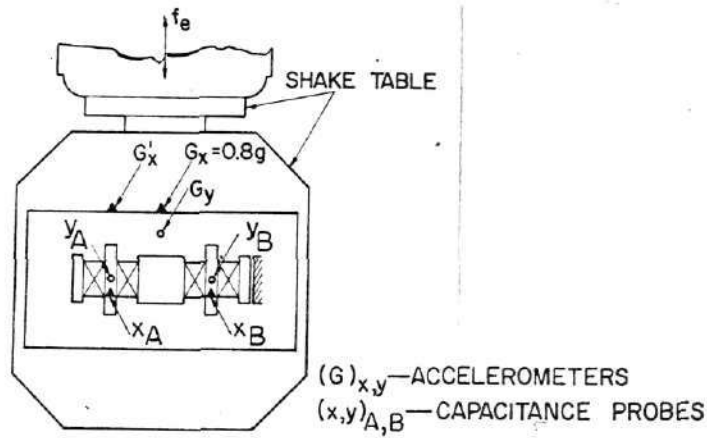
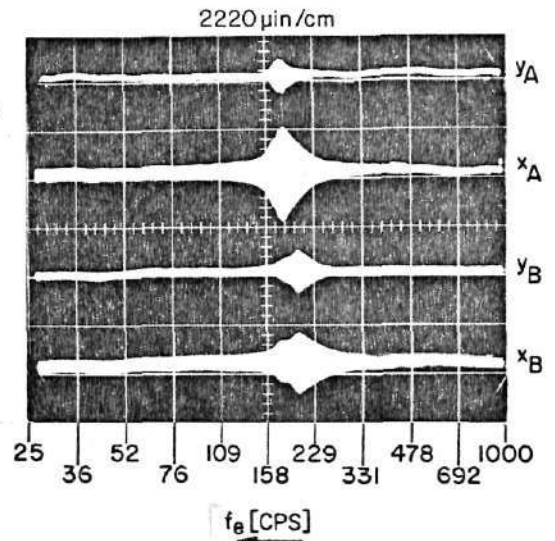
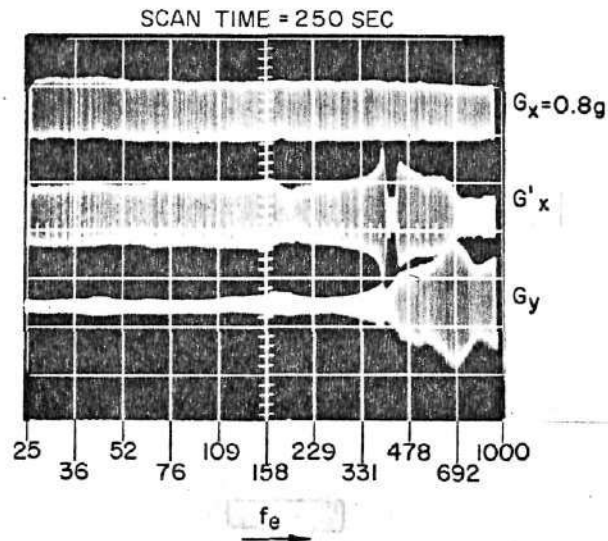
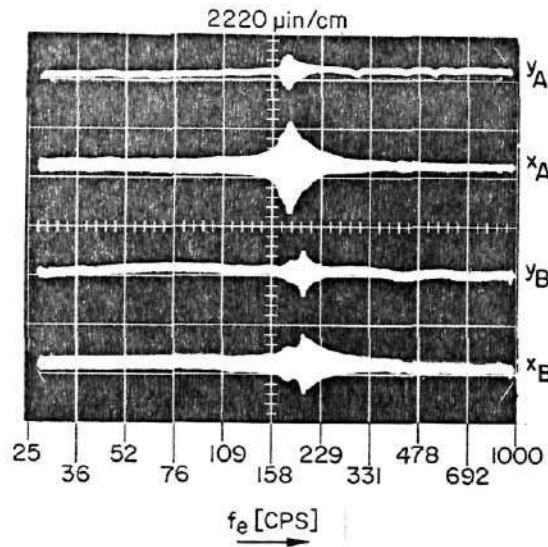
11. Variation of Gap Width with Increasing and Decreasing Speed in the Pressurized and Self-Acting Modes (Vertical Attitude - Foil Sector B₁₃)



12. Comparison of Coastdown Curves in Vertical and Horizontal Attitudes

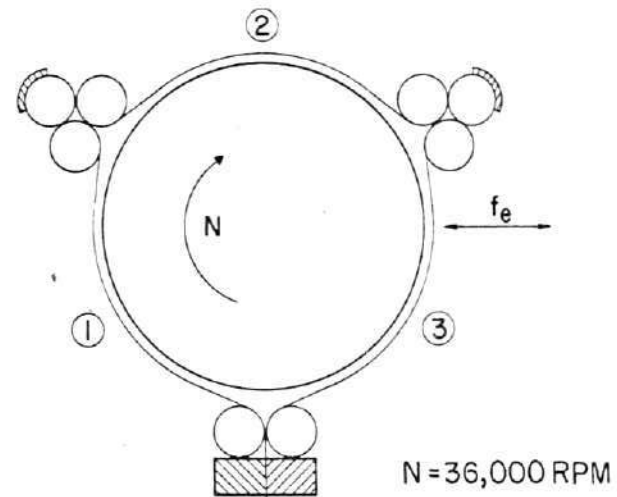
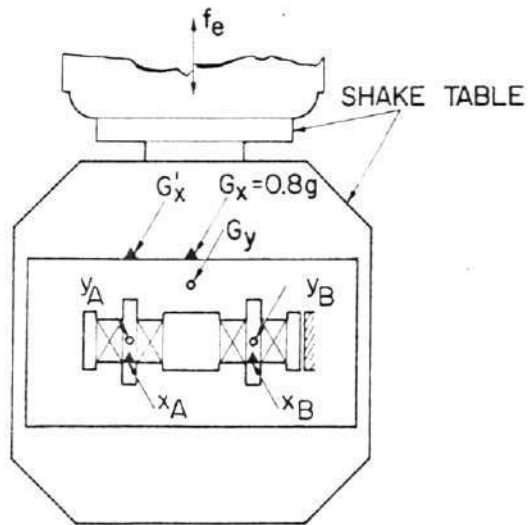
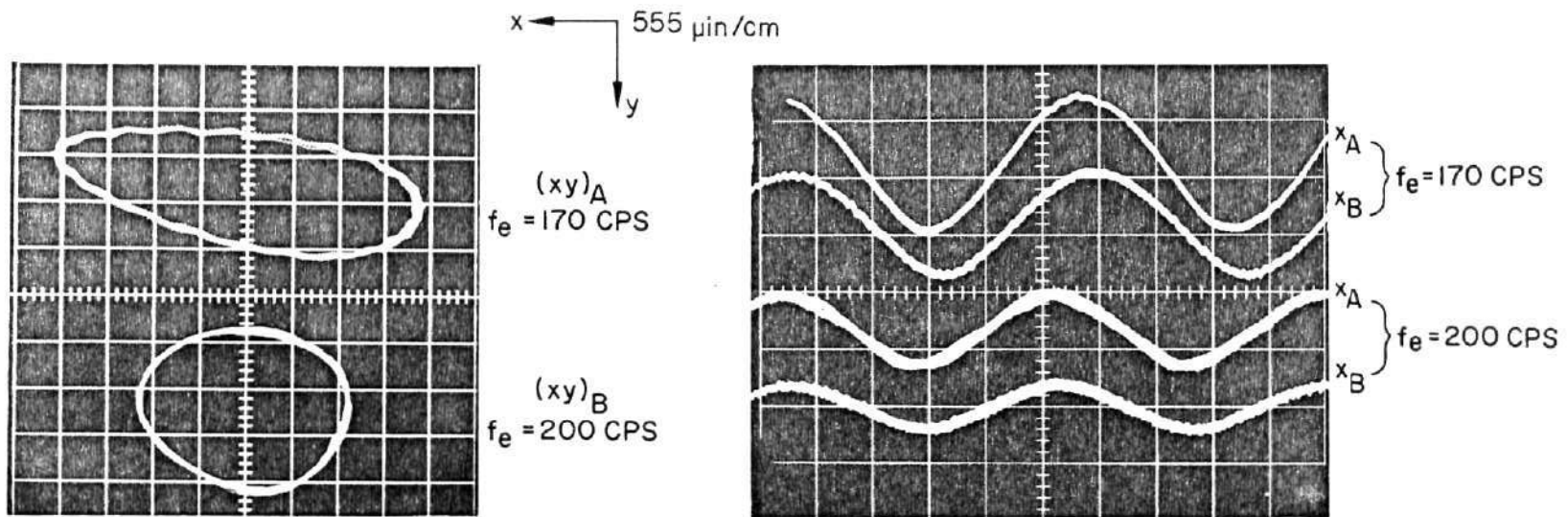


13. View of Experimental Apparatus and Vibrator



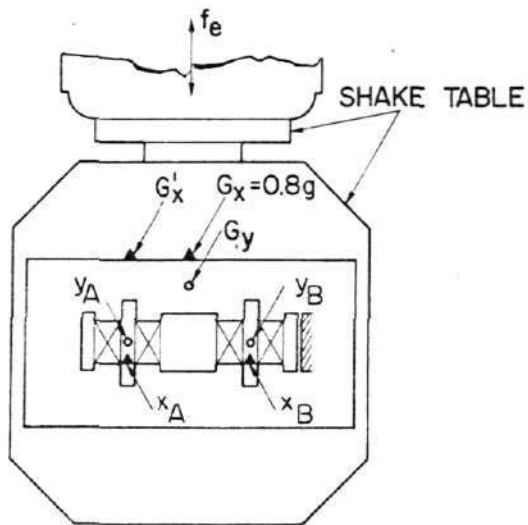
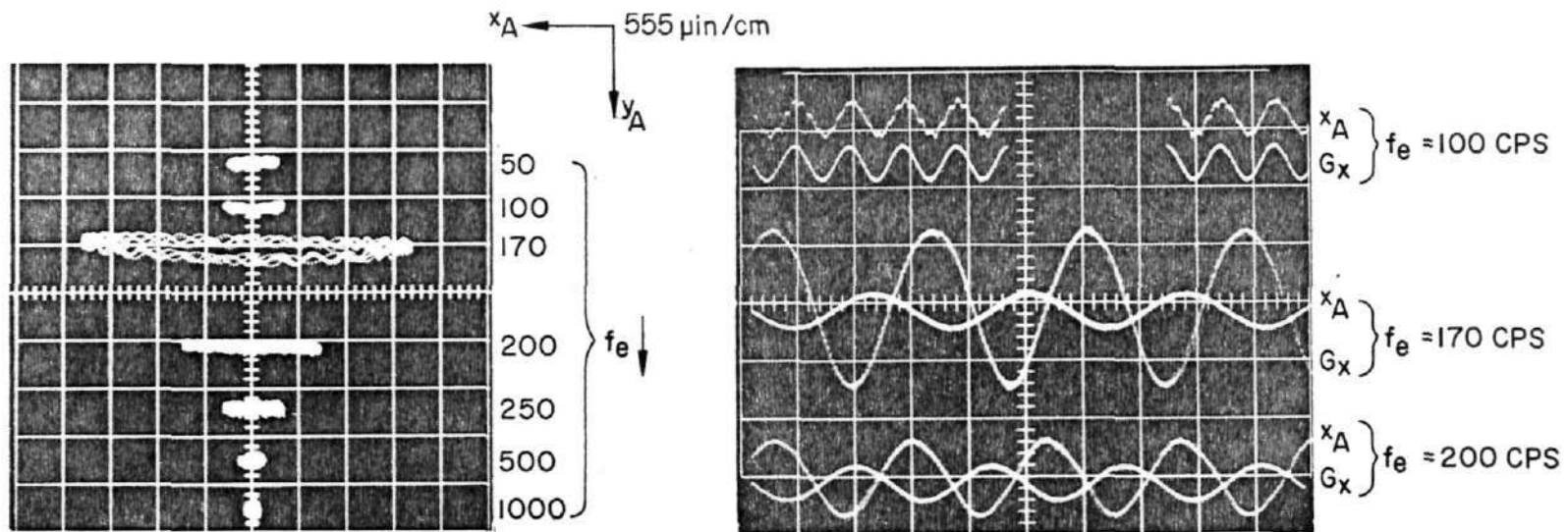
NOT REPRODUCIBLE

14. Scan of Response to Unidirectional Excitation (Horizontal Attitude;

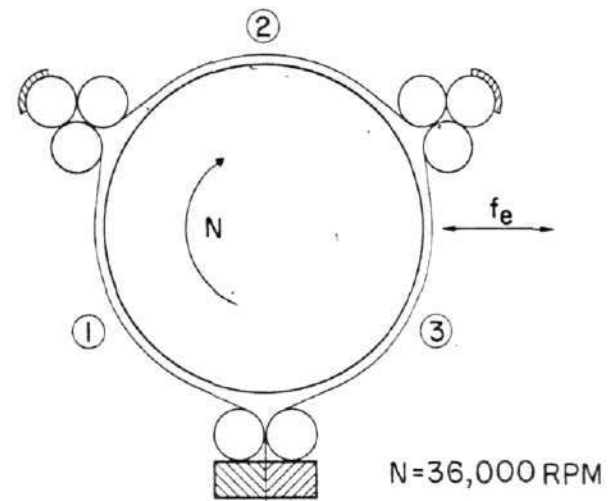


NOT REPRODUCIBLE

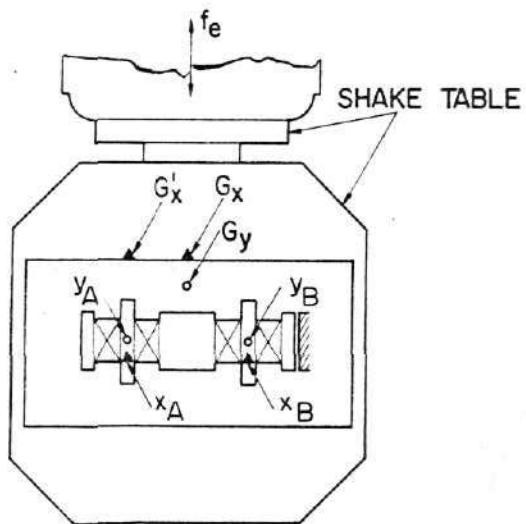
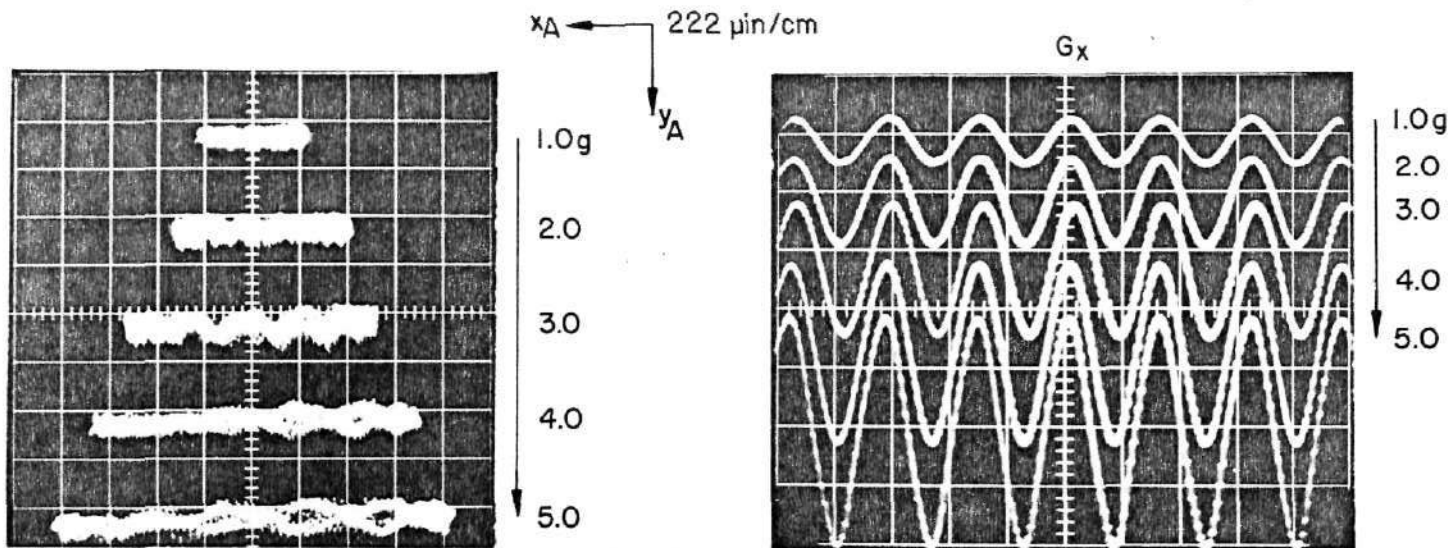
15. Motion of Rotor at Resonance (Horizontal Attitude; $N = 36,000 \text{ RPM}$;



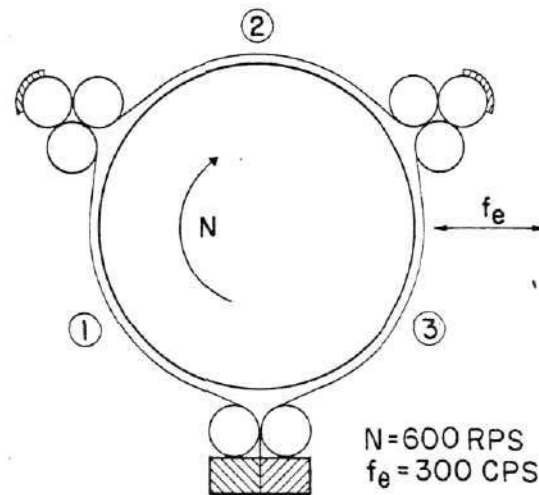
NOT REPRODUCIBLE



16. Motion of Rotor at Various Frequencies of Excitation (Horizontal



NOT REPRODUCIBLE



17. Response of Rotor at Variable Level of Excitation (Horizontal Attitude;